Supplemental Information for

Measurement Report: Spatiotemporal variability of peroxy acyl nitrates (PANs) over Mexico City from TES and CrIS satellite measurements

Madison J. Shogrin[1], Vivienne H. Payne[2], Susan S. Kulawik[3], Kazuyuki Miyazaki[2], and Emily V. Fischer[1]

[1]Colorado State University, Department of Atmospheric Science, Fort Collins, CO, USA

[2]Jet Propulsion Laboratory, California Institute of Technology, Pasadena CA, USA

[3]Bay Area Environmental Research Institute, Petaluma, CA, USA

Correspondence to: Kazuyuki Miyazaki (kazuyuki.miyazaki@jpl.nasa.gov) for supplemental information

S1 Simulations

We used the global chemical transport model, MIROC-CHASER (Sudo et al., 2002; Sekiya et al., 2018; Watanabe et al., 2011), to explain the 3-dimensional distribution of PAN, including the relative contributions of different NO_x emission sources. The model calculates tracer transport (advection, cumulus convection, and vertical diffusion), emissions, dry and wet deposition, and chemical processes (92 species and 262 reactions) of chemical species in the troposphere and stratosphere at 1.125° horizontal resolution. Lightning NO_x sources were calculated in conjunction with the convection scheme of MIROC–atmospheric general circulation model (AGCM) (Watanabe et al., 2011) using the Price and Rind (1992) scheme. The meteorological fields were calculated using the MIROC-AGCM, in which the simulated meteorological fields were nudged to the six-hourly ERA-Interim reanalysis data.

NO_x emissions for 2017 were obtained from an assimilation of multi-species satellite observations (ozone, CO, NO_2, HNO_3, and SO_2) in the Tropospheric Chemistry Reanalysis version 2 (TCR-2) framework (Miyazaki et al., 2020; https://doi.org/10.25966/9qgv-fe81). The tropospheric NO_2 column retrievals from the QA4ECV version 1.1 level 2 products for OMI and GOME-2 (Boersma et al., 2017a, 2017b) were used to constrain NO_x emissions. A priori emissions were obtained from HTAP version 2 for 2010 (Janssens-Maenhout et al., 2015), Global Fire Emissions Database (GFED) version 4 (Randerson et al., 2018), and the Global Emissions Inventory Activity (Graedel et al., 1993) emissions. The data assimilation optimizes only the combined total emission. After the data assimilation, the ratio of different emission categories within the a priori emissions was applied to the estimated emissions to obtain the a posteriori emissions for each sector separately. The quality of the reanalysis fields has been evaluated against independent observations for various chemical species on regional and global scales (Miyazaki et al., 2020).

S2 Simulations of PAN over Mexico City

The CTM model simulations were used to provide an extended picture of PAN variations over the MCMA region, including its vertical profiles and attributions to different emission sources. The general seasonal pattern of the simulated PAN in the troposphere, with a clear maximum in boreal spring in the lower troposphere (up to 1.2 ppb at 750 hPa) (Fig. 9a), is

generally consistent with the observed changes in average tropospheric PAN mixing ratio. Meanwhile, the simulated PAN reveals different seasonal patterns between the lower and upper troposphere, with a maximum concentration of 0.25 ppb in July in the upper troposphere (at 400 hPa) (Fig. 9b), due to atmospheric transports and chemical transformations. This confirms that the observed average tropospheric PAN concentrations from satellites reflect complex vertical structures.

The model sensitivity calculations, by using each NO_x emission source separately, indicate that the enhanced PAN concentrations in the lower troposphere in boreal spring are mostly dominated (>90 %) by anthropogenic sources (Figs. 9 and 10). The continued enhancements from the surface through upper levels suggest the dominant effects from local anthropogenic sources. Biomass burning also increases PAN in April-May, but with smaller contributions than anthropogenic emissions. Soil NOx emissions also have non-negligible impacts. In particular, the local maximum in the upper troposphere during July-August produced by soil emissions demonstrates the importance of natural emissions from surrounding areas on urban PAN distributions. The contributions of lightning emissions are small over MCMA, while it has greater influences over the southern tropics (not shown). The natural emission sources reveal strong interannual variabilities, which could explain parts of the observed multi-year changes. Note that, because of the non-linear chemistry, the sum of each contribution in the sensitivity calculations does not match the total contribution. The model simulation also suggested a broader impact of anthropogenic NO_x emissions from Mexico City in the free troposphere horizontally (not shown). Further insights into the impacts of urban emissions on regional and global nitrogen cycles can be obtained by utilizing global satellite measurements of PAN combined with CTMs and chemical data assimilation (Miyazaki et al., 2020a) in following studies.

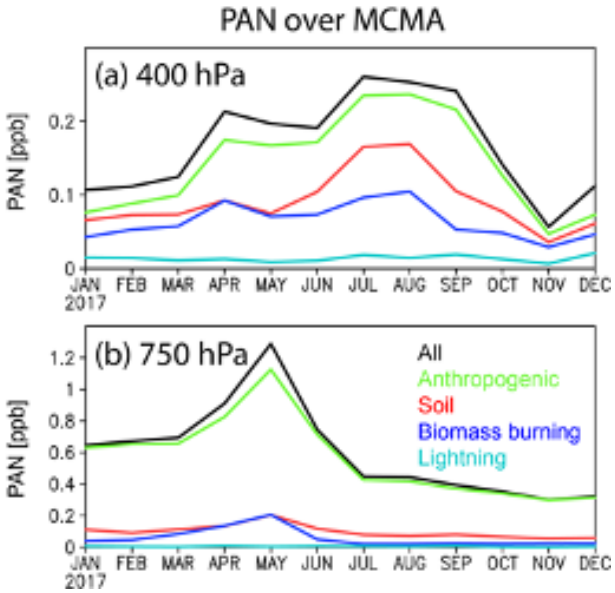

Figure S1. Seasonal changes of monthly mean PAN concentrations (in ppbv) at 750 and 400 hPa over MCMA in 2017 simulated by the CTM (black lines). Results from sensitivity calculations by using each NO_x emission separately are also shown by color lines.

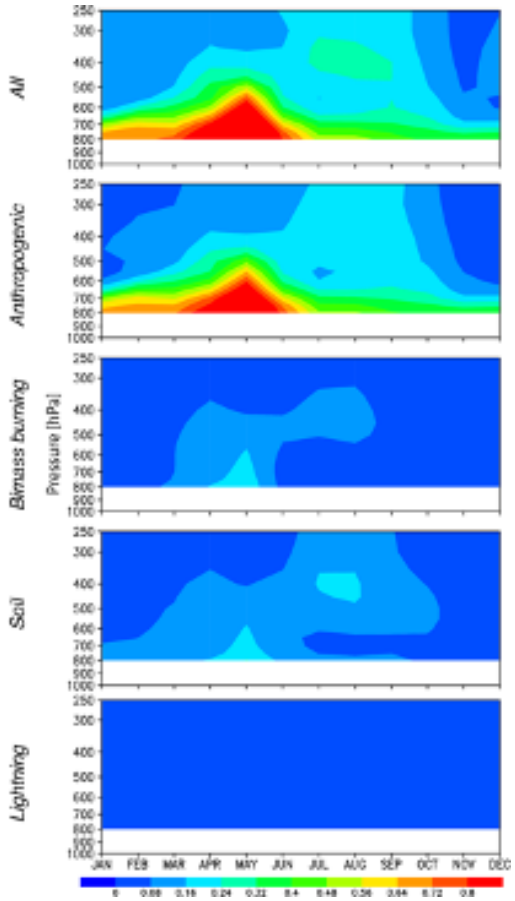

Figure S2. Latitude-pressure cross sections of monthly mean PAN concentrations (in ppbv) over MCMA in 2017 simulated by the CTM (first row). The relative contributions from each emission source separately are also shown (second through fifth row).

References

Boersma, K. F., Eskes, H., Richter, A., De Smedt, I., Lorente, A., Beirle, S., Van Geffen, J., Peters, E., Van Roozendael, M. and Wagner, T., (2017).
QA4ECV NO2 tropospheric and stratospheric vertical column data from OMI (Version 1.1) [Data set]. Royal Netherlands Meteorological Institute (KNMI). http://doi.org/10.21944/qa4ecv-no2-omi-v1.1

Boersma, K. F., Eskes, H., Richter, A., De Smedt, I., Lorente, A., Beirle, S., Van Geffen, J., Peters, E., Van Roozendael, M. and Wagner, T., (2017).

QA4ECV NO2 tropospheric and stratospheric vertical column data from GOME-2A (Version 1.1) [Data set]. Royal Netherlands Meteorological Institute (KNMI). http://doi.org/10.21944/qa4ecv-no2-gome2a-v1.1

Sudo, K., Takahashi, M., Kurokawa, J.-I., and Akimoto, H.: CHASER: A global chemical model of the troposphere 1. Model description, J. Geophys. Res.-Atmos., 107, 4339, https://doi.org/10.1029/2001JD001113, 2002. a

Sekiya, T., Miyazaki, K., Ogochi, K., Sudo, K., and Takigawa, M.: Global high-resolution simulations of tropospheric nitrogen dioxide using CHASER V4.0, Geosci. Model Dev., 11, 959–988, https://doi.org/10.5194/gmd-11-959-2018, 2018.

Watanabe, S., Hajima, T., Sudo, K., Nagashima, T., Takemura, T., Okajima, H., Nozawa, T., Kawase, H., Abe, M., Yokohata, T., Ise, T., Sato, H., Kato, E., Takata, K., Emori, S., and Kawamiya, M.: MIROC-ESM 2010: model description and basic results of CMIP5-20c3m experiments, Geosci. Model Dev., 4, 845–872, https://doi.org/10.5194/gmd-4-845-2011, 2011.

Miyazaki, K., Eskes, H., Sudo, K., Boersma, K. F., Bowman, K., and Kanaya, Y.: Decadal changes in global surface NO_x emissions from multi-constituent satellite data assimilation, Atmos. Chem. Phys., 17, 807–837, https://doi.org/10.5194/acp-17-807-2017, 2017.

Miyazaki, K., Bowman, K., Sekiya, T., Eskes, H., Boersma, F., Worden, H., Livesey, N., Payne, V. H., Sudo, K., Kanaya, Y., Takigawa, M., and Ogochi, K.: Updated tropospheric chemistry reanalysis and emission estimates, TCR-2, for 2005–2018, Earth Syst. Sci. Data, 12, 2223–2259, https://doi.org/10.5194/essd-12-2223-2020, 2020.

Price, C. and Rind, D.: A simple lightning parameterization for calculating global lightning distributions, J. Geophys. Res.-Atmos., 97, 9919–9933, 1992

Janssens-Maenhout, G., Crippa, M., Guizzardi, D., Dentener, F., Muntean, M., Pouliot, G., Keating, T., Zhang, Q., Kurokawa, J., Wankmüller, R., Denier van der Gon, H., Kuenen, J. J. P., Klimont, Z., Frost, G., Darras, S., Koffi, B., and Li, M.: HTAP_v2.2: a mosaic of regional and global emission grid maps for 2008 and 2010 to study hemispheric transport of air pollution, Atmos. Chem. Phys., 15, 11411–11432, https://doi.org/10.5194/acp-15-11411-2015, 2015.

Randerson, J., van der Werf, G., Giglio, L., Collatz, G., and Kasibhatla, P.: Global Fire Emissions Database, Version 4, (GFEDv4), ORNL DAAC, Oak Ridge, Tennessee, USA, https://doi.org/10.3334/ORNLDAAC/1293, 2018.

Graedel, T. E., Bates, T. S., Bouwman, A. F., Cunnold, D., Dignon, J., Fung, I., Jacob, D. J., Lamb, B. K., Logan, J. A., Marland, G., Middleton, P., Pacyna, J. M., Placet, M., and Veldt, C.: A compilation of inventories of emissions to the atmosphere, Global Biogeochem. Cy., 7, 1–26, 1993